Bioorganic & Medicinal Chemistry Letters 20 (2010) 5803–5806

Contents lists available at ScienceDirect

Bioorganic & Medicinal Chemistry Letters

journal homepage: www.elsevier.com/locate/bmcl

Pyrazolopyridines as potent PDE4B inhibitors: 5-Heterocycle SAR

Charlotte J. Mitchell *, Stuart P. Ballantine, Diane M. Coe, Caroline M. Cook, Christopher J. Delves, Mike D. Dowle, Chris D. Edlin †, J. Nicole Hamblin, Stuart Holman, Martin R. Johnson, Paul S. Jones, Sue E. Keeling, Michael Kranz, Mika Lindvall ‡, Fiona S. Lucas, Margarete Neu, Yemisi E. Solanke, Don O. Somers, Naimisha A. Trivedi, Joanne O. Wiseman

GlaxoSmithKline, Medicines Research Centre, Gunnels Wood Road, Stevenage, Hertfordshire, SG1 2NY, United Kingdom

ARTICLE INFO

Article history:
Received 16 June 2010
Revised 28 July 2010
Accepted 30 July 2010
Available online 5 August 2010

Keywords:
PDE4 inhibitor
Pyrazolopyridine
SAR

ABSTRACT

Following the discovery of 4-(substituted amino)-1-alkyl-pyrazolo[3,4-b]pyridine-5-carboxamides as potent and selective phosphodiesterase 4B inhibitors, [Hamblin, J. N.; Angell, T.; Ballentine, S., et al. *Bioorg. Med. Chem. Lett.* **2008**, *18*, 4237] the SAR of the 5-position was investigated further. A range of substituted heterocycles showed good potencies against PDE4. Optimisation using X-ray crystallography and computational modelling led to the discovery of **16**, with sub-nM inhibition of LPS-induced TNF-α production from isolated human peripheral blood mononuclear cells.

Phosphodiesterase 4 (PDE4) is an enzyme responsible for the inactivation of cyclic adenosine monophosphate (cAMP), via hydrolysis to 5′-AMP. Inhibition of PDE4 results in an elevation of cAMP, which in turn downregulates the inflammatory response. PDE4 is the predominant phosphodiesterase enzyme present in inflammatory cells (e.g., neutrophils, monocytes, macrophages)[2] and in addition is a key regulator of cAMP metabolism in airway epithelial cells.[3] It is therefore established as an interesting target for the treatment of respiratory diseases such as chronic obstructive pulmonary disease (COPD).[4]

First generation PDE4 inhibitors exemplified by Rolipram **1** (Fig. 1), demonstrated severe side effects of nausea and emesis at effective anti-inflammatory doses.[5] Whilst second generation PDE4 inhibitors such as Roflumilast **2** (Fig. 1) have shown improved side effect profiles in clinical trials, the maximum dose is still limited by adverse events.[6]

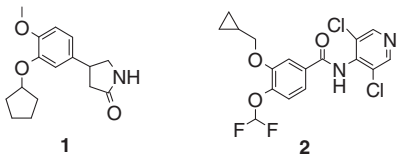

1 **2**

Figure 1. Structures of Rolipram and Roflumilast.

Our aim was therefore to identify a third generation of PDE4 inhibitors, which could provide a greater therapeutic window between efficacy in COPD treatment and emetic side effects.

We have previously described the identification of pyrazolopyridine (PZP) **3**[1] (Fig. 2), which showed inhibition of isolated PDE4B[7] and lipopolysaccharide (LPS) induced tumour necrosis factor alpha (TNF-α) production in human peripheral blood mononuclear cells (PBMCs).[8]

Further work to explore the structure–activity relationship (SAR) around the PZP template led us to investigate the replacement of the 5-amide group with a range of heterocycles, initially 1,3,4- and 1,2,4-oxadiazoles.

In each case the heterocyclic rings were synthesized from key intermediate **4**. For the 1,3,4-oxadiazoles, the ester was first

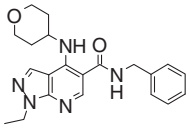

3
PDE4B pIC50 8.5
PBMC pIC50 7.7

Figure 2. Pyrazolopyridine 5-carboxamide.

* Corresponding author. Tel.: +44 1438 762542; fax +44 1438 7683022.
E-mail address: charlotte.j.mitchell@gsk.com (C.J. Mitchell).
† Present address: iThemba Pharmaceuticals, Pinelands Site, Ardeer Road, Building T5, Modderfontein 1609, Gauteng, South Africa.
‡ Present address: Novartis Institute for Biomedical Research, 4560 Horton Street, Emeryville, CA 74607, USA.

0960-894X/$ - see front matter © 2010 Elsevier Ltd. All rights reserved.
doi:10.1016/j.bmcl.2010.07.136

converted to hydrazide **5** by hydrolysis, coupling with BOC-hydrazine and deprotection under acidic conditions. Subsequent acylation under standard conditions to give the diacyl hydrazide **6**, followed by cyclisation with Burgess reagent,[9] gave the desired targets **7a–f** (Scheme 1).

In cases where the carboxylic acid required for conversion of **5** to **6** was not available, the targets were synthesized from key acid and amine intermediates **8** and **9** (Scheme 2).

For the 1,2,4-oxadiazoles **10a–f**, intermediate **4** was reacted in a one pot procedure with a range of amidoximes to give the desired products directly. Alternatively **4** was first hydrolysed to carboxylic acid **11**, coupled with the amidoxime and cyclised with DBU (Scheme 3). Where the appropriate amidoximes were not available these could be synthesized from the corresponding nitrile, by reaction with hydroxylamine.[10]

As with the 1,3,4- series, some analogues were prepared via a key amine intermediate **12** (Scheme 4).

Preliminary structure–activity studies were conducted against isolated PDE4B,[11] the predominant PDE4 sub-type in inflammatory cells of interest.[12] Results indicated that both oxadiazole isomers were tolerated at the 5-position (Table 1). Different oxadiazole substituents showed optimum potency in each series but no general trend to rank one isomer above the other was observed.

For example, benzyl substituted analogues **7b/10b** and pyrrolidine amides **7d**/**10d** showed similar potencies in both series,

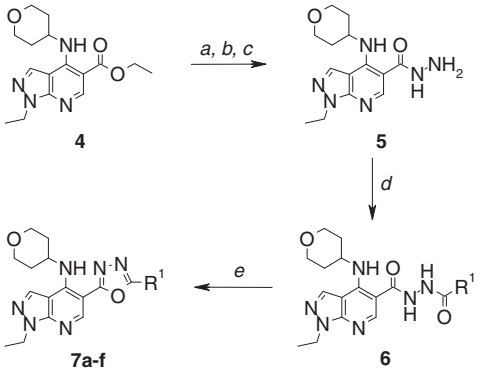

Scheme 1. Reagents and conditions: (a) NaOH, EtOH/H_2O, 18 h (99%); (b) $NH_2NHCO_2{}^tBu$, EDC, HOBt, DMF, 18 h (82%); (c) 4 M HCl, 1,4-dioxane, 2 h (100%); (d) R^1COOH, TBTU, DIPEA, DMF, 18 h; (e) Burgess reagent, THF, 75 °C, 2 h.

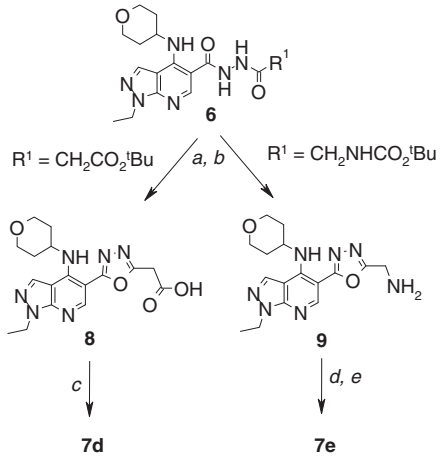

Scheme 2. Reagents and conditions: (a) Burgess reagent, THF, 75 °C, 2 h (70%); (b) TFA, DCM, 4 h (100%); (c) Pyrrolidine, pybop, DIPEA, DMF, 18 h (43%); (d) 4-chlorobutanoyl chloride, DIPEA, MeCN, 1 h; (e) NaH, DMF, 2 h (43% over two-steps).

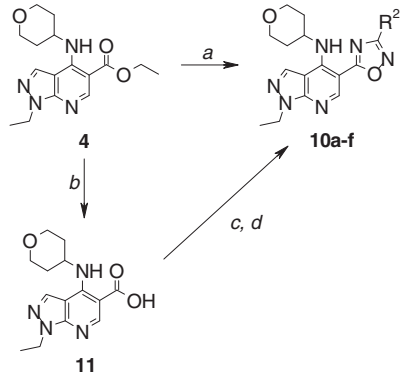

Scheme 3. Reagents and conditions: (a) $R^2C(NOH)NH_2$, NaOEt, molecular sieves, 75 °C, 18 h; (b) NaOH, EtOH/H_2O, 18 h (99%); (c) $R^2C(NOH)NH_2$, TBTU, HOBt, DIPEA, DMF, 20 h; (d) DBU, DMF, 85 °C, 0.75 h.

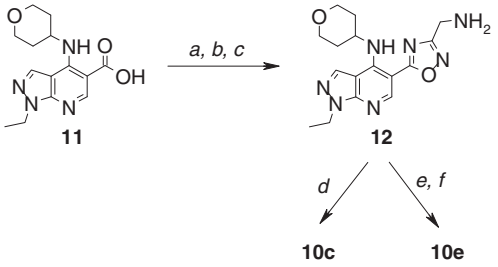

Scheme 4. Reagents and conditions: (a) $^tBuOC(O)CH_2C(NOH)NH_2$, TBTU, HOBt, DIPEA, DMF, 2 h; (b) DBU, DMF, 85 °C, 3.5 h (89% over two steps); (c) TFA, DCM, 0 °C, 2 h (99%); (d) MeCOCl, DIPEA, DCM, 16 h (96%); (e) 4-chlorobutanoyl chloride, DIPEA, MeCN, 16 h; (f) NaH, DMF, 16 h (83% over two-steps).

Table 1
SAR of 1,3,4-oxadiazoles **7a–f** and 1,2,4-oxadiazoles **10a–f**

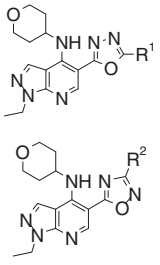

	R^1	PDE 4B pIC_{50}[a]	PBMC pIC_{50}[a]		R^2	PDE 4B pIC_{50}[a]	PBMC pIC_{50}[a]
7a	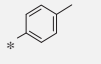	8.9[b]	NT	**10a**	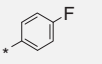	8.0[b]	NT
7b	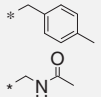	8.0[b]	8.3	**10b**	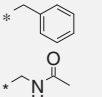	8.2[b]	7.5
7c	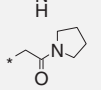	7.3	NT	**10c**	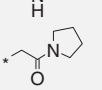	8.1[b]	NT
7d	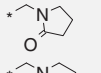	8.7[b]	NT	**10d**	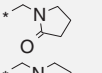	9.1[b]	NT
7e	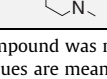	8.4[b]	7.0	**10e**	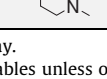	9.4[b]	8.5
7f	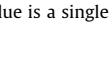	7.3	6.9	**10f**		7.8[b]	NT

NT Compound was not progressed to PBMC assay.
[a] Values are mean of ⩾2 experiments in all tables unless otherwise stated.
[b] Value is a single experiment.

whereas, the pyrrolidinone substituted 1,2,4-oxadiazole **10e** showed ~10-fold improvement over 1,3,4-oxazdiazole **7e**.

For both isomers a range of functionalities gave good potencies suggesting manipulation of the substituent might offer a useful means of varying physicochemical properties.

For selected analogues, inhibition of LPS-induced TNF-α production in isolated human PBMCs was also measured (Table 1). Generally both series of oxadiazole showed similar or improved potency in the PBMC assay to 5-amide **3**.

Computational modelling in the PDE4 active site suggested that the binding mode of the oxadiazoles would vary between isomers, rationalizing the observed divergent SAR. The five-membered heterocycles were suggested to be coplanar with the PZP ring system, fixed by an intramolecular H-bond to the NH of the 4-aminotetrahydropyran substituent. Their conformational preferences are determined by the superior acceptor strength of the oxadiazole nitrogen over that of the oxygen[13] (Fig. 3).

Whilst the 1,3,4-oxadiazole R^1 substituents were predicted to occupy the same pocket as the N substituent in the 5-amide series (Fig. 4), the 1,2,4-oxadiazole R^2 substituents were expected to access a different pocket, previously unfilled.

The binding mode of the 1,2,4-isomer was confirmed by X-ray crystallography of **10d** (Fig. 5) which clearly revealed the direction of the oxadiazole substituent.[1] It is wedged between Ser-282 and Met-347 and also in van der Waals contact with the PZP's 4-THP. The pyrrolidine amide can adopt two conformations, only one of which is shown in Figure 5, the other one occupies a similar region with an 180° amide rotation leading to a close contact between the pyrrolidine ring and Cys-432 as well as Phe-414.

Using this information we decided to investigate oxazoles as an alternative heterocyclic core. Whilst 4- and 5-mono-substituted oxazoles were expected to mimic, respectively, the 1,2,4- and 1,3,4-oxadiazoles already synthesized, di-substituted oxazoles had the potential to fill both pockets with the aim of increasing PDE4B potency even further (Fig. 6).

Using SAR from the two oxadiazole series, di-substituted oxazole **16** was designed. A benzyl group was chosen as the R^1 substituent (well tolerated in the 1,3,4-oxadiazole **7b**) and a pyrrolidine amide was introduced at R^2 (cf. **10d** in the 1,2,4-oxadiazole series).

Synthesis proceeded from key intermediate **13**. Amide coupling followed by a Dakin–West reaction[14] with the appropriate anhydride led to desired intermediate **14**, which was cyclised using phosphorous oxychloride as a dehydrating agent. Basic hydrolysis of the ester, followed by amide formation gave the desired product **16** (Scheme 5).

For completeness, mono-substituted oxazole **18** was also synthesized. Amide coupling of key pyrazolopyridine intermediate **11** with 1-amino-3-phenyl-2-propanol, followed by oxidation of the alcohol gave intermediate **17**. Subsequent cyclisation with Burgess reagent gave the desired 5-substituted oxazole **18** (Scheme 6).

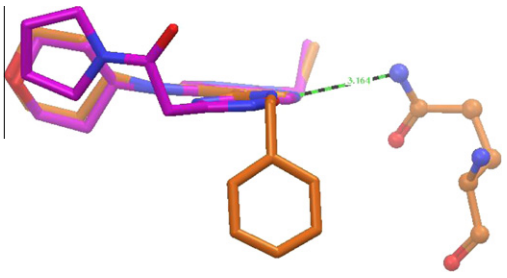

Figure 5. Overlay of X-ray crystal structures of 5-amide **3** (orange) and 1,2,4-oxadiazole **10d** (magenta) (only Glu443 shown for clarity).

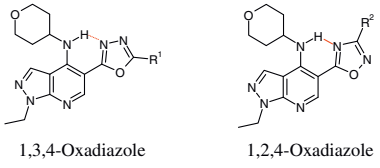

Figure 3. Orientation of 1,3,4- and 1,2,4-oxadiazoles relative to PZP core (red lines represent H-bonding interactions).

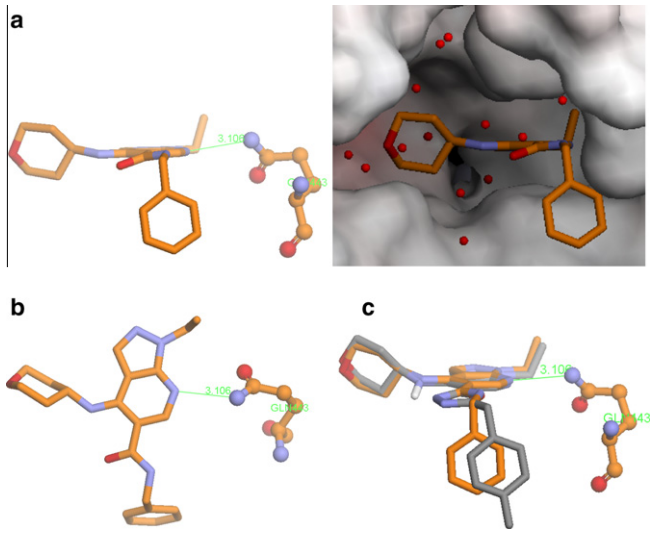

Figure 4. (a) X-ray crystal structure of 5-amide **3** in PDE4 active site (with and without protein surface); (b) X-ray crystal structure of 5-amide **3** rotated 90° (only Glu443 shown for clarity); (c) X-ray crystal structure of 5-amide **3** (orange) overlaid with computational model of 1,3,4-oxadiazole **7b** (grey).

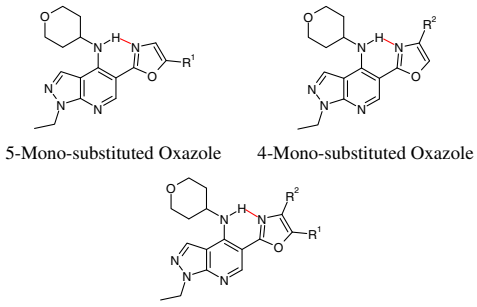

Figure 6. Orientation of oxazoles.

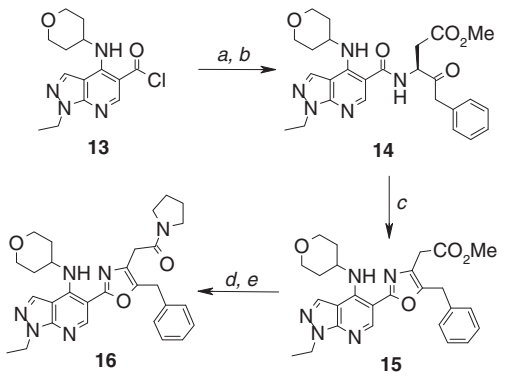

Scheme 5. Reagents and conditions: (a) (*S*)-$NH_2C(CO_2H)CH_2CO_2Me$, py, 7 h; (b) $(PhCH_2CO)_2O$, reflux, 5 h; (c) $POCl_3$, toluene, 120 °C, 23 h; (d) LiOH, THF/H_2O, 40 °C, 1 h; (e) pyrrolidine, HATU, DIPEA, MeCN, 8 h.

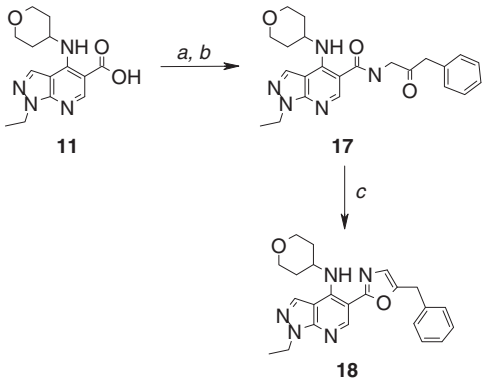

Scheme 6. Reagents and conditions: (a) $PhCH_2C(OH)CH_2NH_2$, HATU, DIPEA, MeCN, 12 h (100%); (b) py.SO_3H, Et_3N, DMSO, 24 h (58%); (c) Burgess reagent, THF, 75 °C, 3 h (50%).

The di-substituted oxazole **16** demonstrated sub-nM activity in the isolated enzyme and PBMC assay (Table 2) and gave at least 10-fold increase in potency over 1,3,4-oxadiazole **7b**, 1,2,4-oxadiazole **10d** (Table 1) and 5-amide **3**. Comparison with the mono-subsituted oxazole **18** also showed an increase in potency on introduction of a second substituent.

An X-ray crystal structure of **16** soaked into a PDE4B crystal was obtained and confirmed the proposed binding mode with both pockets occupied, rationalizing the improved potencies observed (Fig. 7).[1] The pyrrolidine amide can again adopt two conformations. The one shown in Figure 7 is the same as for the 1,2,4-oxadiazole in Figure 5, the other one involves an 180° flip of the amide so the carbonyl is pointing in the opposite direction but the pyrrolidone ring remains in the same position.

In summary, exploration of the SAR around lead pyrazolopyridine **3**, led us to 5-heteorcyclic compounds exemplified by **7b** and **10d**. Following promising PDE4 potency shown with these initial analogues, computational modelling and X-ray crystallography were employed to fully optimise ligand–protein interactions. The design of 4,5-disubstituted oxazoles gave **16** which occupied two key pockets in the active site, resulting in a significant increase in potency.

Table 2
SAR of oxazoles

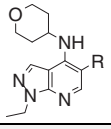

Compd	R	PDE4B pIC_{50}	PBMC pIC_{50}
3	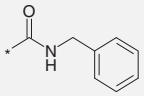	8.5[b]	7.7
16	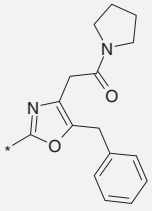	10.1	9.6
18	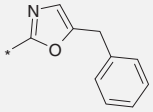	8.6[a]	8.0

[a] Value is a single experiment.
[b] Data from an alternative assay format.[7]

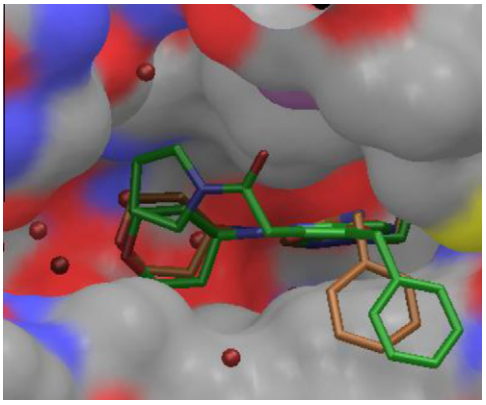

Figure 7. Overlay of X-ray crystal structures of 5-amide **3** (orange) and di-substituted oxazole **16** (cyan) with protein surface shown.

The success of these ligands in achieving an improved therapeutic index in vivo will be the subject of further papers.

Acknowledgements

The authors thank Damien Charre and Violaine Werquin for their synthetic contributions whilst on placement at GSK.

References and notes

1. Methods according to Hamblin, J. N.; Angell, T.; Ballentine, S., et al *Bioorg. Med. Chem. Lett.* **2008**, *18*, 4237. except compound **10d** was soaked into an apo-PDE4B crystal at 1 mM for ~2 days, while compound **16** was soaked at 2 mM for ~1 day. Data were collected for compound **16** at station 17ID-B of the Advanced Photon Source (Argonne, USA) using an ADSC Q210 CCD detector. During refinement, the occupancy of **16** was set at 0.7 to account for incomplete soaking of the compound into the crystal probably due to poor compound solubility. The final R-factors achieved for the complexes **10d** and **16** following structure refinement were 19.6% (R_{free} = 26.0%) and 18.7% (R_{free} = 24.0%), respectively, and the coordinates deposited in the PDB as entries 3O56 and 3O57.
2. Torphy, T. J.; Undem, B. J. *Thorax* **1991**, *46*, 512.
3. Torphy, T. J.; Undem, B. J.; Cieslinski, L. B.; Luttmann, M. A.; Reeves, M. L.; Hay, D. W. P. *J. Pharmacol. Exp. Ther.* **1993**, *265*, 1213.
4. McKenna, J. M.; Muller, G. W. *Cyclic Nucleotide Phosphodiesterases in Health and Disease*; CRC Press: LLC, Boca Raton, Florida ,USA, 2007; Dyke, Hazel J. *Expert Opin. Ther. Pat.* **2007**, *17*, 1183; Smith, V. B.; Spina, D. *Curr. Opin. Invest. Drugs* **2005**, *6*, 1136.
5. Horowski, R.; Sastre-Y-Hernandez, M. *Curr. Ther. Res.* **1998**, *38*, 23.
6. Rabe, F.; O'Donnell, D.; Muir, F., et al *Eur. Respir. J.* **2004**, *24*. Abstr. 267.
7. The ability of compounds to inhibit catalytic activity of PDE4B (human recombinant) was determined by scintillation proximity assay (SPA) in 96-well format as described in WO2004024728.
8. The ability of compounds to inhibit LPS induced TNF-α production in PBMCs was determined by electrochemiluminescence using the Meso Scale Discovery (MSD) technology as described in WO 2007036733.
9. Ersmark, K.; Nervall, M.; Hamelink, E., et al *J. Med. Chem.* **2005**, *48*, 6090.
10. Sahbari, J.; Russell, J. WO0032565.
11. The ability of compounds to inhibit catalytic activity at PDE4B (human recombinant) was determined by IMAP Fluorescence Polarisation (FP) assay (IMAP Explorer kit, available from Molecular Devices Corporation, Sunnydale, CA, USA; Molecular Devices code: R8062) in 384-well format as described in WO 2004056823.
12. Wang, P.; Ohelth, K. M.; Wu, P.; Billah, M. M.; Egan, R. W. *Mol. Pharmacol.* **1999**, *56*, 170.
13. The 4-methylamino-3-oxadiazole-pyridine model systems show a clear preference for the nitrogen coordination to the amino NH_{**}over the oxygen coordination for the 1,2,4- (2.8 kcal/mol at B3LYP/6-31+G) and the 1,3,4-oxadiazoles (6.2 kcal/mol).
14. Buchanan, G. L. *Chem. Soc. Rev.* **1988**, *17*, 91.